THREE-DIMENSIONAL BOUNDARY ELEMENT ANALYSIS OF FIBRE/MATRIX INTERFACE CRACKS

Jhonny E. Ortiz and Adrián P. Cisilino

División Soldadura y Fractomecánica - INTEMA
Facultad de Ingeniería – Universidad Nacional e Mar del Plata
Avda Juan B. Justo 4302, 7600 Mar del Plata, Argentina
e-mail: cisilino@fi.mdp.edu.ar

Palabras clave: interface cracks, boundary elements, composite materials

Abstract. *It is presented in this work a general numerical tool for the analysis of three-dimensional bimaterial interface cracks. The proposed tool is based on a multidomain formulation of the Boundary Element Method (BEM), with the crack located at the interface. Mixed-mode stress intensity factors along three-dimensional bimaterial interface cracks are computed using M_1-Integral methodology, which imposes the asymptotic auxiliary fields for the plane problem of a bimaterial interface crack along the crack front. The M_1-integral is evaluated using a domain representation naturally compatible with the BEM, since stresses, strains and derivatives of displacements at internal points can be evaluated using the appropriate boundary integral equations. The capability of the procedure is demonstrated by solving an application example, namely the analysis of a fibre/matrix debond interface crack under transverse loading.*

1   INTRODUCTION

The overall mechanical properties of composite materials depend heavily on the nature of the bond at bimaterial interfaces. Unfortunately, interfacial delamination and fracture are commonly observed problems that may ultimately limit the use of these materials, which range from ceramic and metal matrix composites for the aerospace industry to nanoscale structures for microelectronics applications. The need to improve fracture their toughness has led to significantly progress in the area of interfacial fracture mechanics. During the past few decades, comprehensive analyses have been carried out, and many questions regarding the mechanics of interface fracture have been answered. However, progress has been generally mainly focused in the two-dimensional idealization of an interface crack, and limited work has been conducted on the three-dimensional aspect of interface fracture. This is in part due to the extreme complexity of such problems and the very large computational efforts required for their numerical analysis. However, given the material mismatch along the interface boundary, it is expected that the three-dimensional effects play a more significant role in a bimaterial structure than in a homogenous structure.

The attraction of the BEM can be largely attributed to the reduction in the dimensionality of the problem; for two-dimensional problems, only the line-boundary of the domain needs to be discretized into elements, and for three-dimensional problems only the surface of the domain needs to be discretized. This means that, compared to FEM domain type analysis, a boundary analysis results in a substantial reduction in data preparation. At the same time, and due to the inherent characteristics of its formulation, the BEM provide very accurate results for problems containing strong geometrical discontinuities. This makes the BEM a powerful numerical tool for modelling crack problems[1].

Although many authors propose displacement and stress extrapolation methods to determine stress intensity factors from BEM results (see for example Tan and Gao[2], Yuuki and Cho[3], Mao and Sun[4] and He W.J., Lin D.S. and Ding H.J[5], *J*-integral methods constitute a more robust approach. Note that BEM is specially suited for the evaluation of path independent integrals, since the required stresses, strains and derivatives of displacements at internal points can be directly obtained from their boundary integral representations. It also has been shown that BEM produces more accurate stresses and strains at internal points when compared with other numerical techniques, and therefore better results can be achieved. Application of the *J*-integral methodology for two-dimensional interface cracks can be found in the work by Miyazaki et al[6] and de Paula and Aliabadi[7].

Among the available schemes for the numerical computation of the J-integral in three dimensions, the Energy Domain Integral (EDI) due to Shih[8] is employed in this work. Previous work by one of the authors has proved the versatility and efficiency of the EDI in the three-dimensional BEM analysis of isotropic cracked bodies[9]. Together with the EDI the interaction or M_1-integral methodology due to Chen and Shield[10] is employed in this work for decoupling the *J*-integral into the mixed-mode stress intensity factors. The M_1-integral methodology is based on the superposition of two equilibrium states, given by the actual problem and a set of auxiliary known solutions. This approach has been recently reported in a number of papers using FEM to compute stress intensity factors along three-dimensional

interface cracks (see Gosz, Dolbow and Moran[11], Nagashima, Omoto and Tani[12], and Im, Kim and Kim[13]. Using BEM the M_l-integral methodology has been implemented for two-dimensional cracks by Miyazaki et al[6].
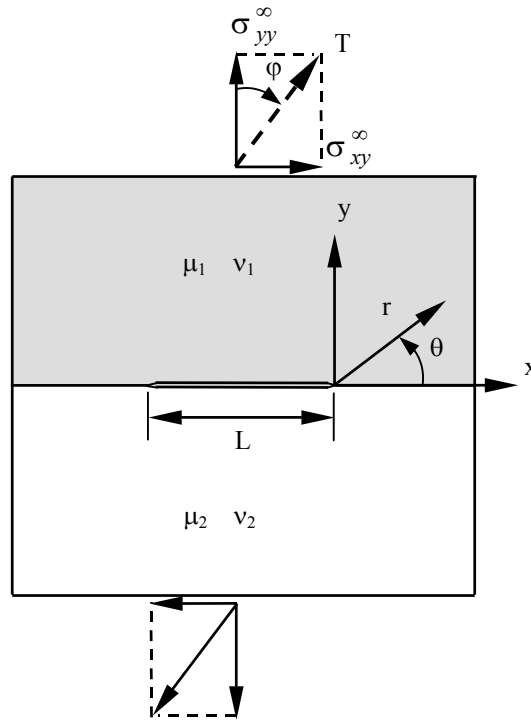
Figure 1: schematic of bimaterial plate with an interface crack: coordinate system in the region of the crack tip and remote tension and shear loading.

2 CRACK TIP FIELD AND BIMATERIAL INTERFACES

Consider the plane problem of an interface crack between two dissimilar isotropic materials as shown in Figure 1. For convenience, we adopt a local polar coordinate system centred at the crack tip, and we label the material occupying the upper half-plane as material 1 with Young modulus E_l and Poisson ratio ν_1. The material occupying the lower half-plane has modulii E_2 and ν_2. The stress field very close to the crack front corresponds to the asymptotic field based on the two-dimensional (plain strain and antiplane) solutions due to Williams[14]. The form of the bimaterial stress field given by Rice, Suo and Wang[15] (with the addition of Mode III) is

$$\sigma_{ij} = \frac{1}{\sqrt{2\pi r}}\left\{\mathrm{Re}\left[\mathbf{K}r^{i\varepsilon}\right]\tilde{\sigma}_{ij}^{I}(\theta;\varepsilon) + \mathrm{Im}\left[\mathbf{K}r^{i\varepsilon}\right]\tilde{\sigma}_{ij}^{I}(\theta;\varepsilon) + K_{III}\tilde{\sigma}_{ij}^{III}(\theta)\right\},\tag{1}$$

where r and θ are the in-plane coordinates of the plane normal to the crack front, $\mathbf{K}$ is defined as the complex stress intensity factor for the in-plane modes, $\mathbf{K} = K_I + iK_{II}$, and $\hat{\sigma}_{ij}$ are the angular variations of stress components for each mode. The oscillatory index ε is

$$\varepsilon = \frac{1}{2\pi} \ln\left[\frac{\kappa_1 \mu_2 + \mu_1}{\kappa_2 \mu_1 + \mu_2}\right] = \frac{1}{2\pi} \ln\left[\frac{1-\beta}{1+\beta}\right]. \tag{2}$$

Here, $\kappa_\alpha = 3 - 4v_\alpha$ for plane strain and $\kappa_\alpha = (3 - v_\alpha)/(1 + v_\alpha)$ for plane stress, $\mu_\alpha = E_\alpha /(1 + v_\alpha)$ is the shear modulus, and the subscripts $\alpha=1,2$ refer to the materials above and bellow the crack plane, respectively. Furthermore, β is one of Dundurs´ parameters. In two-dimensional problems, the solution can be characterized by the two Dundurs´ parameters, and they are defined as[16]:

$$\alpha = \frac{\mu_1(\kappa_2 + 1) - \mu_2(\kappa_1 + 1)}{\mu_2(\kappa_1 + 1) + \mu_1(\kappa_2 + 1)}, \quad \beta = \frac{\mu_1(\kappa_2 - 1) - \mu_2(\kappa_1 - 1)}{\mu_2(\kappa_1 + 1) + \mu_1(\kappa_2 + 1)}. \tag{3}$$

Unlike the two-dimensional cases, the above parameters are not sufficient to characterize the full-field field deformation of three dimensional boundary value problems. Note, a bimaterial combination yields different Dundurs´ parameters under plain-strain and plane-stress conditions.

3 THE INTERACTION INTEGRAL

The M_I-integral is based on the principle of superposition. Let us consider two equilibrium states with field variables denoted by the superscripts (1) and (2), respectively. Superposition of the two equilibrium states leads to another one, (1+2). Then the stress intensity factors $K_j^{(1+2)}$ can be written as

$$K_j^{(1+2)} = K_j^{(1)} + K_j^{(2)} \quad (j = I, II, III). \tag{6}$$

The stress intensity factors can be related to the J-integral for the superimposed state (1+2) for a crack at the interface between two dissimilar isotropic materials under plain strain conditions as follows[11]:

$$J^{(1+2)} = \frac{1}{E^* \cosh^2(\pi\varepsilon)}\left[\left(K_I^{(1+2)}\right)^2 + \left(K_{II}^{(1+2)}\right)^2\right] + \frac{1}{2\mu^*}\left(K_{III}^{(1+2)}\right)^2 \tag{7}$$

where E^* and μ^* are the effective Young´s and shear modulus[11,] and ε stands for the bimaterial constant defined in Eq. (2). Equation (7) can be rewritten in terms of the stress intensity factors for the equilibrium states (1) and (2), to give

$$J^{(1+2)} = J^{(1)} + J^{(2)} + \frac{2}{E^* \cosh^2(\pi\varepsilon)}\left[K_I^{(1)} K_I^{(2)} + K_{II}^{(1)} K_{II}^{(2)}\right] + \frac{1}{2\mu^*} K_{III}^{(1)} K_{III}^{(2)}. \tag{8}$$

Then, the M_I-integral is defined as

$$M_1 = J^{(1+2)} - J^{(1)} - J^{(2)} = \frac{2}{E^* \cosh^2(\pi\varepsilon)} \left[K_I^{(1)} K_I^{(2)} + K_{II}^{(1)} K_I^{(2)} \right] + \frac{1}{2\mu^*} K_{III}^{(1)} K_{III}^{(2)} . \tag{9}$$

Finally, the M_I-integral can be expressed using a domain representation using the energy domain integral approach[17]

$$M_1 = \int_V \left(\sigma_{ij}^{*(1)} u_{j,k}^{*(2)} + \sigma_{ij}^{*(2)} u_{j,k}^{*(1)} - \sigma_{ij}^{*(1)} \varepsilon_{ij}^{*(2)} \delta_{ki} \right) q_{,i} dV . \tag{10}$$

For the decoupling the mixed-mode stress intensity factors, the problem under consideration is selected as equilibrium state (1), so that the field variables $\sigma_{ij}^{*(1)}$ and $u_{j,k}^{*(1)}$ will be obtained in this work from the results of a boundary element analysis. On the other hand, the plain-strain solutions for the asymptotic crack-tip fields introduced in Section 1 with prescribed stress intensity factors K_I, K_{II} and K_{III}, are selected as equilibrium state (2). Then the field variables related with the equilibrium state (2), $\sigma_{ij}^{*(2)}, u_{j,k}^{*(2)}$ and $\varepsilon_{ij}^{*(2)}$ are calculated from these asymptotic solutions. Finally the M_I-integral defined in Eq.(10) can be calculated, using the field variables related with the equilibrium states (1) and (2). By using three sets of asymptotic solutions, ($K_I^{(2)} = 1, K_{II}^{(2)} = 0, K_{III}^{(2)} = 0$), ($K_I^{(2)} = 0, K_{II}^{(2)} = 1, K_{III}^{(2)} = 0$) and ($K_I^{(2)} = 0, K_{II}^{(2)} = 0, K_{III}^{(2)} = 1$), it is possible to obtain the stress intensity factor solutions for individual modes from Eq.(9) as follows:

$$K_I^{(1)} = \frac{E^* \cosh^2(\pi\varepsilon)}{2} M_1^a$$

$$K_{II}^{(1)} = \frac{E^* \cosh^2(\pi\varepsilon)}{2} M_1^b \tag{11}$$

$$K_{III}^{(1)} = \frac{E^* \cosh^2(\pi\varepsilon)}{2} M_1^c$$

where M_1^a, M_1^b and M_1^c are the values of the M_I-integral calculated using the three sets of asymptotic solutions.

It is important to point out that the present implementation of the M_I-integral approach is only valid for straight crack fronts. For the application of the M_I-integral along curved crack fronts extra terms need to be included in Eq.(10). At he same time it is worth to note that because the M_I-integral is based upon the assumption that the near-crack tip fields asymptote to the plane strain fields, it is not strictly applicable at the intersection of the crack front with a free surface. It turns that out that at the intersection of the crack front and the free surface, the singularity in the stress field is more severe than the usual $1/\sqrt{r}$ singularity[18].

4 MULTIDOMAIN BEM FORMULATION

Considering a body with domain $\Omega(X)$ surrounded by a boundary $\Gamma(x)$ (see Figure 2a), the displacement boundary integral equation relating the boundary displacements $u(x)$ with the boundary traction $t(x)$ in the absence of body forces can be written for three-dimensional problem as,

$$c_{ij}(x')u_i(x') + \int_\Gamma T_{ij}^*(x',x)u_j(x)d\Gamma(x) = \int_\Gamma U_{ij}^*(x',x)t_j(x)d\Gamma(x) \quad i,j = 1,2,3 \tag{12}$$

where $T_{ij}^*(x',x)$ and $U_{ij}^*(x',x)$ are, respectively, the fundamental displacement and traction solutions due to a unit load placed at a location x'. These solutions are provided in Ref.[1].
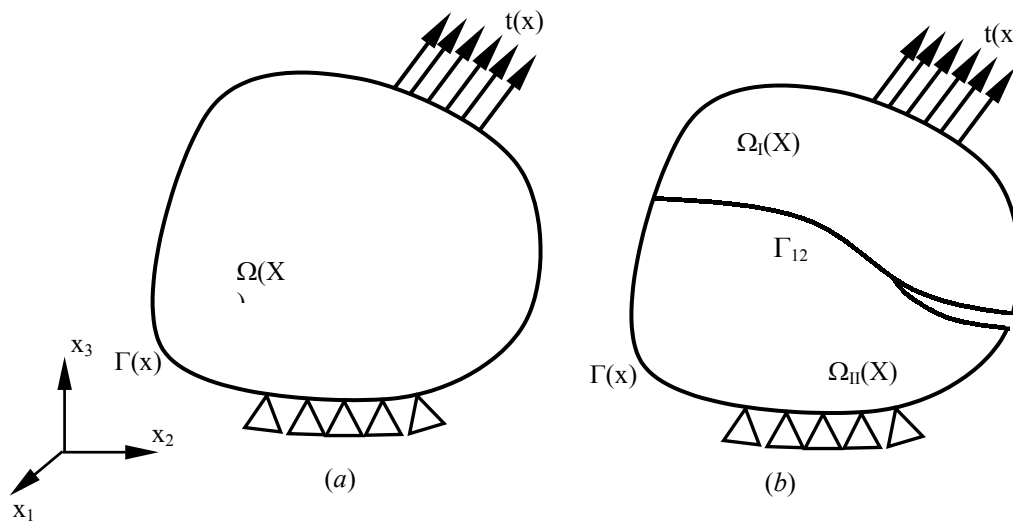
Figure 2: (a) Three dimensional body with volume Ω and boundary Γ, (b) Schematic of the multidomain technique for nonhomogeneous body.

Because Eq.(12) is derived for a homogeneous material, a multidomain technique is used to solve the interface crack problems. As shown in Figure 4b, the whole domain is divided into two domains $\Omega_I(X)$ and $\Omega_{II}(X)$, which are both homogeneous. The boundary element technique is applied to each domain resulting in the following matrix equations

$$\left[\mathbf{H}_1^I \ \mathbf{H}_2^I \right] \begin{Bmatrix} \mathbf{u}_1^I \\ \mathbf{u}_2^I \end{Bmatrix} = \left[\mathbf{G}_1^I \ \mathbf{G}_2^I \right] \begin{Bmatrix} \mathbf{t}_1^I \\ \mathbf{t}_2^I \end{Bmatrix} \tag{13a}$$

for domain *I*, and

$$\begin{bmatrix} \mathbf{H}_1^{II} \ \mathbf{H}_2^{II} \end{bmatrix} \begin{Bmatrix} \mathbf{u}_1^{II} \\ \mathbf{u}_2^{II} \end{Bmatrix} = \begin{bmatrix} \mathbf{G}_1^{II} \ \mathbf{G}_2^{II} \end{bmatrix} \begin{Bmatrix} \mathbf{t}_1^{II} \\ \mathbf{t}_2^{II} \end{Bmatrix} \qquad (13b)$$

for domain *II*. Matrices **H** and **G** in Eqs. (13) contain integrals of the kernel functions $T_{ij}^*(x',x)$ and $U_{ij}^*(x',x)$ respectively, while **u** and **t** are vectors with the nodal displacements and tractions on the boundary. Here the subscript 2 indicates the common interface boundary Γ_{12} of each domain (see Figure 2), while subscript 1 stands for the rest of the boundary. If the equilibrium and continuity conditions are enforced at the common interface give

$$u_2^I = u_2^{II} \qquad (14a)$$

and

$$t_2^I = -t_2^{II} . \qquad (14b)$$

Incorporating Eqs. (14*a*) and (14*b*) into Eqs. (13*a*) and (13*b*) results in the following matrix equations:

$$\begin{bmatrix} \mathbf{H}_1^I & \mathbf{H}_2^I & 0 \\ 0 & \mathbf{H}_2^{II} & \mathbf{H}_1^{II} \end{bmatrix} \begin{Bmatrix} \mathbf{u}_1^I \\ \mathbf{u}_2^I \\ \mathbf{u}_1^{II} \end{Bmatrix} = \begin{bmatrix} \mathbf{G}_1^I & \mathbf{G}_2^I & 0 \\ 0 & -\mathbf{G}_2^{II} & \mathbf{G}_1^{II} \end{bmatrix} \begin{Bmatrix} \mathbf{t}_1^I \\ \mathbf{t}_2^I \\ \mathbf{t}_1^{II} \end{Bmatrix} \qquad (15)$$

The problem boundary conditions are then applied to the system of equation (15). If the displacements are known on certain portion of the model boundary the traction can be found and vice versa. This implies that the system of Eq.(15) can be reordered in such a way that all the unknowns are written on the left hand-side vector resulting in

$$[\mathbf{A}][\mathbf{x}] = [\mathbf{y}] \qquad (16)$$

where **x** is the vector of unknown displacement and traction boundary values including the common interface.
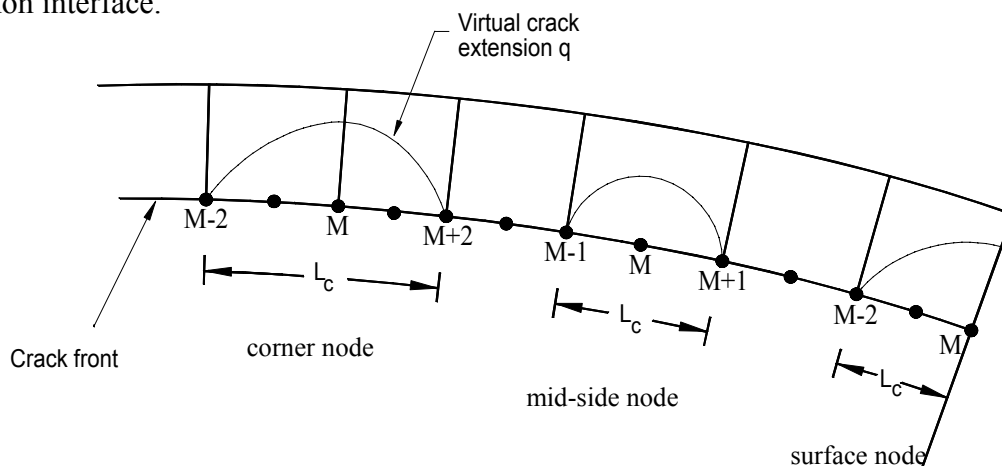
Figure 3: Schematic of the volume cells in the crack front region illustrating the virtual crack extensions for a corner node, a mid-node and a surface node.

5 BOUNDARY ELEMENT IMPLEMENTATION

The computation of the M_I-integral methodology was implemented in the BEM code as a post-processing procedure, and so it could be applied to the results from a particular model at a later stage. This procedure requires the evaluation of a volume integral within closed domains that enclose a segment of the crack front L_c. A natural choice here is to make the evaluation point η coincident with the element nodes on the crack front, while L_c is taken as the element or element sides at which points η lies (see Figure 3). The portion of the model domain in which the volume integrals are evaluated is discretized using 27-noded isoparametric (brick) cells, over which stresses, strains and displacements derivatives are approximated by products of the cell interpolation functions Ψ_i and the nodal values of σ_{ij}, ε_{ij} and $u_{i,j}$. Volume discretization is designed to have a web-style geometry around the crack front, while the integration volumes are taken to coincide with the different rings of cells. This is illustrated in Figure 4, where one of the model faces has been removed to show the crack and the integration domains. The procedures for the computation of the nodal values for σ_{ij}, ε_{ij} and $u_{i,j}$ are the same to those employed in Ref[9].

crack face

crack front

interface

integration domains

(a)   (b)
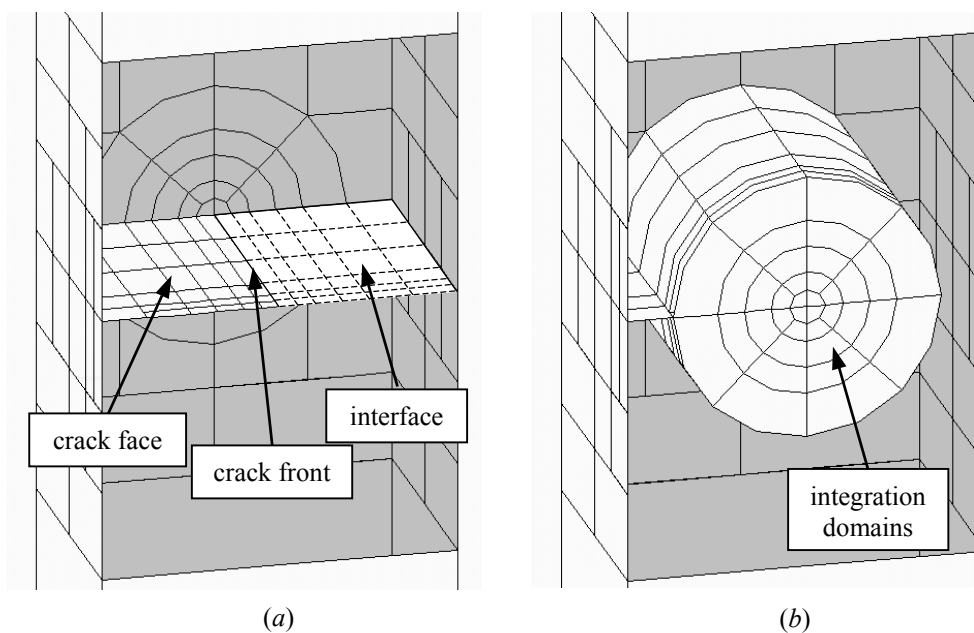
Figure 4: (a) Boundary Element discretization, (b) Integration domains

In this work q is defined to vary quadratically in the directions tangential and normal to the crack front. This bi-quadratic definition of q has been employed with excellent results in the computation of EDI for cracks in homogeneous materials in a previous work by one of the authors[9]. Within this approach, and considering that the evaluation point η is at the middle of the crack front segment L_c, and r_0 is the radius of the integration domain, the function q is written as:

$$q(x^*) = \left| 1 - \left(\frac{x_3^*}{L_C / 2} \right)^2 \right| \cdot \left[1 - \left(\frac{r}{r_0} \right)^2 \right] \qquad (17)$$

where x_3^* is the distance from the evaluation point η in the local direction tangential to the crack front.

Function q is specified at all nodes within the integration volumes. Consistent with the isoparametric formulation, these q-values are given by

$$q = \sum_{i=1}^{27} \Psi_i Q^i \qquad (18)$$

where Ψ_i are the shape functions defined within each volume cell and Q^i are the nodal values for the ith node.

If Gaussian integration is used, the discretized forms for the M_1-integral is given by

$$M_1 = \sum_{cells\ in\ V} \sum_{p=1}^{m} \left\{ \left(\sigma_{ij}^{*(1)} u_{j,k}^{*(2)} + \sigma_{ij}^{*(2)} u_{j,k}^{*(1)} - \sigma_{ij}^{*(1)} \varepsilon_{ij}^{*(2)} \delta_{ki} \right) q_{,i}\ \det \left(\frac{\partial x_j}{\partial \zeta_k} \right) \right\}_p w_p \qquad (19)$$

respectively, where m is the number of Gaussian points per cell, and w_p are the weighting factors.

6 APPLICATION EXAMPLE: FIBRE/MATRIX INTERFACE CRACK UNDER TRANSVERSE LOADING

6.1 Boundary Element Model

Figure 5 illustrates the strategy proposed for the idealization of the BEM model. Figure 5(a) corresponds to a micrograph in the direction transversal to the fibres in unidirectional glass/epoxy laminate. It can be observed that although the fibres are distributed almost homogeneously, there are regions of the laminate that are rich in matrix. It is assumed in this work that the fibres are packed in a periodic square array, and that the damage takes place in one of the fibres by a pair of symmetric cracks running circumferentially between the fibre and the matrix (see Figure 5(b)). At the same time the behaviour of the remaining portion of the laminate is idealized as transversely isotropic, with its isotropy plane perpendicular to the direction of the fibres (plane xy in the figure). This results in a BEM model composed by three regions with two planes of symmetry as depicted in Figure 5(c). Regions I and II (isotropic) are used to model the representative volume element given by the fibre and the matrix around it, while Region III (transversely isotropic) models the effect of the remaining portion of the laminate and provides boundary conditions to the zone of interest.
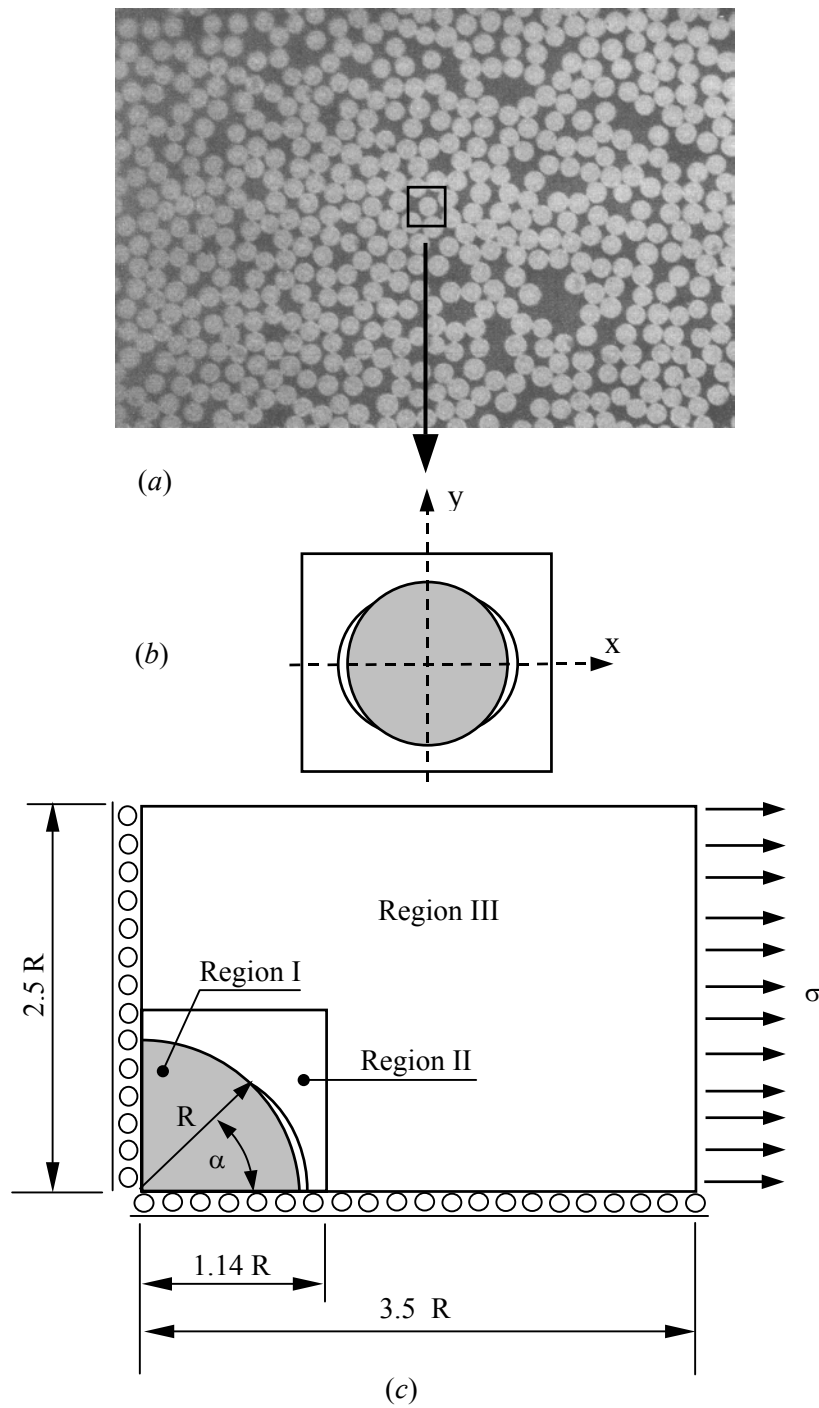
Figure 5: Schematics of the BEM model: (*a*) micrograph in the direction transversal to the fibres in unidirectional glass/epoxy laminate , (*b*) square cell with symmetric debond cracks, (*c*) model dimensions and boundary conditions

Model dimensions are given in Figure 5(c) as a function of the radius of the fibre R, and in such a way that the fibre volume fraction represents 60% of the representative volume element. Model thickness is $t = 1.5\ R$. The debond angle is selected $\alpha = 37°$ in order to avoid the crack face contact. Elastic properties of the fibre are $E_f = 7.80\ 10^{10}$ MPa and $v_f = 0.22$, and $E_m = 2.79\ 10^9$ MPa and $v_m = 0.33$ for the matrix. The oscillatory index for this bimaterial combination is $\varepsilon = 0.074$. The properties for the transversely isotropic material are $E_1 = 8.9\ 10^9$ MPa and $v_1 = 0.27$, and $E_2 = 43\ 10^9$ MPa and $v_2 = 0.06$ for the isotropy plane and the direction of the fibres respectively. The discretized model geometry is illustrated in Figure 6. It consists of 291 elements and 1353 nodes. Forty-nine elements are used for the crack face discretization. Four rings of cells with radii r/a = 0.18, 0.28, 0.39 and 0.46 are employed for J-integral and stress intensity factor computations. The number of cells used with this purpose is 252.
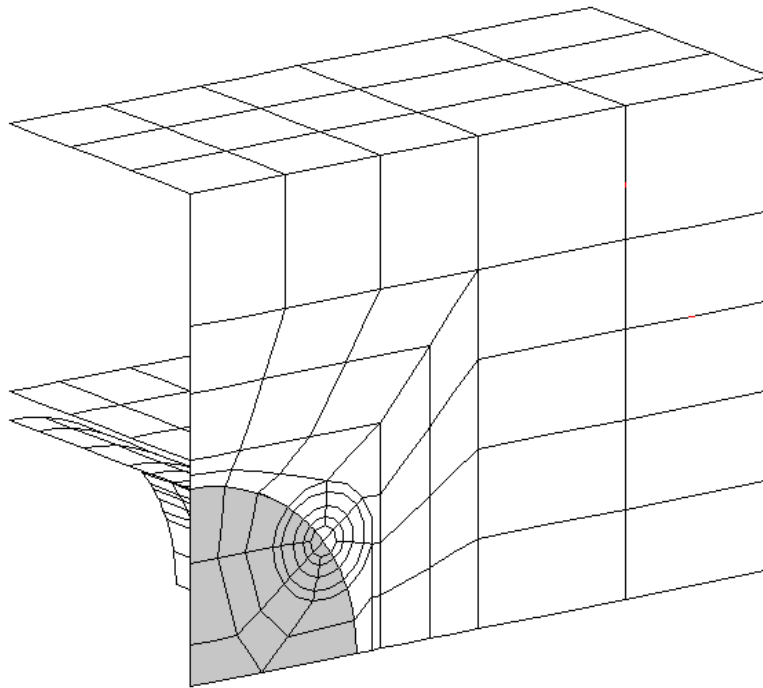
Figure 6: Boundary element model for the fibre/matrix interface crack

The model is analysed considering five different material combinations. The first case is devised for validation purposes and to allow comparison with two-dimensional results. With this idea all the three regions of the model are considered isotropic and with identical material properties (note that this assumption reduces the problem to that of a circular arc crack in an homogeneous panel). At the same time the displacements in the direction of the thickness restricted in order to obtain plane strain conditions. The other four cases are devoted to study the influence of the material properties of Region III on the fibre/matrix interface crack behaviour. Thus, in the second case the event of single fibre in a homogeneous panel is

considered, and so the elastic properties for Region III are set identical to those of the matrix material (Region II). Cases three to five assume a transversely isotropic behaviour for Region III. In case three, elastic properties of Region III are those of the glass/epoxy laminate given in the previous paragraph, while cases four and five consider the two limiting cases for which the elastic properties of the isotropy plane coincide with those of the fibre ($E_I = E_f$, $\nu_I = \nu_f$) and the matrix ($E_I = E_m$, $\nu_I = \nu_m$) respectively.

6.2 Results and discussion

J-integral results obtained along the crack front for the five material combinations are plotted in Figure 7. The origin of the normalized coordinate *z/t* corresponds to the specimen mid-plane, and all values are normalized with respect to the *J*-integral result for a crack in an infinite bimaterial plate $J_o=(K)^2/[E^*cosh^2(\pi\varepsilon)]$, where $K=\sigma^\infty[(1+4\varepsilon^2)\pi a]^{1/2}$ and E^* is the effective elastic modulus for the fibre/matrix bimaterial combination. As it is expected, the plane-strain homogeneous model results in a constant *J*-integral value along the complete crack front. On the other hand, the model of the single fibre presents the most marked variation along the crack front, with its largest value at the free surface (*z/t*=0.5). If the effect of the fibres in the laminate is considered (results labelled as "fibre in laminate" in Figure 7), the large stiffness of the specimen in the direction of the thickness makes the crack to behave as in the plain strain model, and a constant *J*-integral value is obtained along the complete crack front. The two other sets of results correspond to the limiting cases for which the elastic properties of the isotropy plane are taken the same to those of the matrix and the fibre respectively. When the elastic properties are those of the matrix, the *J*-integral value is almost the same to that obtained for the single fibre example at the interior of the specimen, but it drops at the free surface. Finally, when the elastic properties of the isotropy plane are those of the fibre (the most rigid of all cases analysed) *J*-integral presents its lowest level, and similarly to the homogeneous case it presents a constant value along the complete crack front. The above results allow explaining experimental observations as those reported by Meurs[19], who tested a single glass-fibre-reinforced specimen in transverse loading and observed that crack initiates at the specimen surface, where the maximum *J*-integral value is achieved. It is also worth to note that this analysis for single fibre can be assimilated to the situation in an actual laminate for which an irregular packing of fibres due to inhomogeneous fibre distribution leads to a zone rich in matrix.

Stress intensity factor results are presented for the three modes of cracking in Figures 8 to 10. Results are normalized with respect to $\sigma^\infty\sqrt{\pi a}$. Figure 8 allows to observe that the behaviour of K_I along the crack front is very similar to that exhibited by the *J*-integral, that is, the maximum K_I values are obtained for the cases with the largest material mismatch between the fibre and the surrounding material (*i.e.* the case of the single fibre, and the limiting case for which the elastic properties of the isotropy plane are taken coincident with those of the matrix). Similar results are obtained for K_{II}, with the only difference that *K* values tend now to increase towards the free surface for both, the case of the single fibre, and when the elastic

properties of the isotropy plane are those of the matrix. It is also worth to note that the K_{II} level for this two cases is very close to that of the two-dimensional homogeneous case.
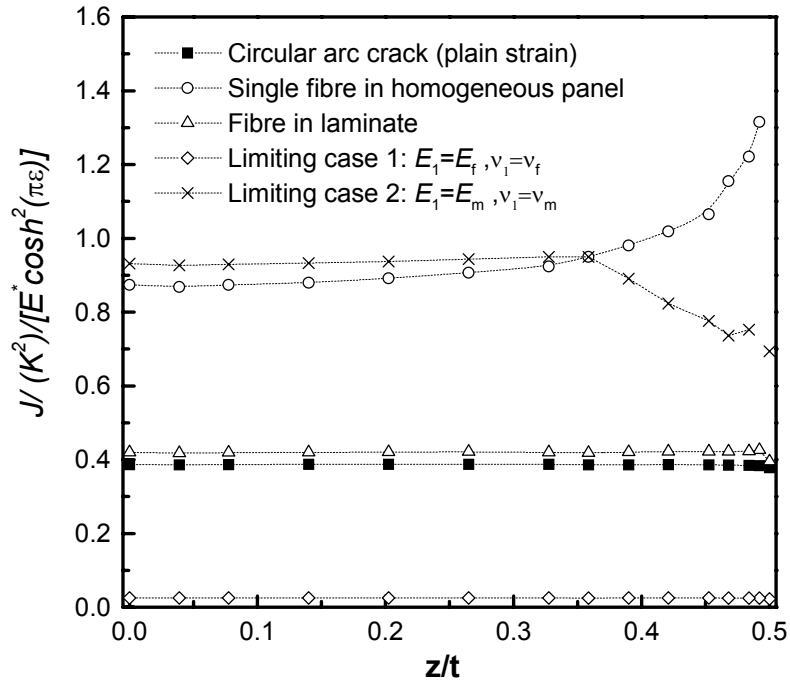
Figure 7: J-integral along the crack front for the fibre/matrix interface crack
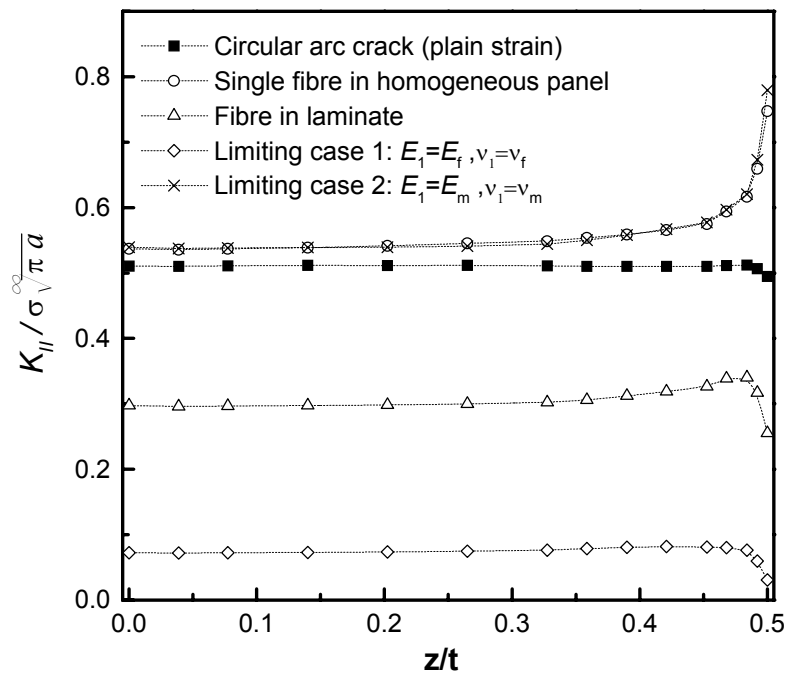
Figure 9: K_{II} along the crack front for the fibre/matrix interface crack
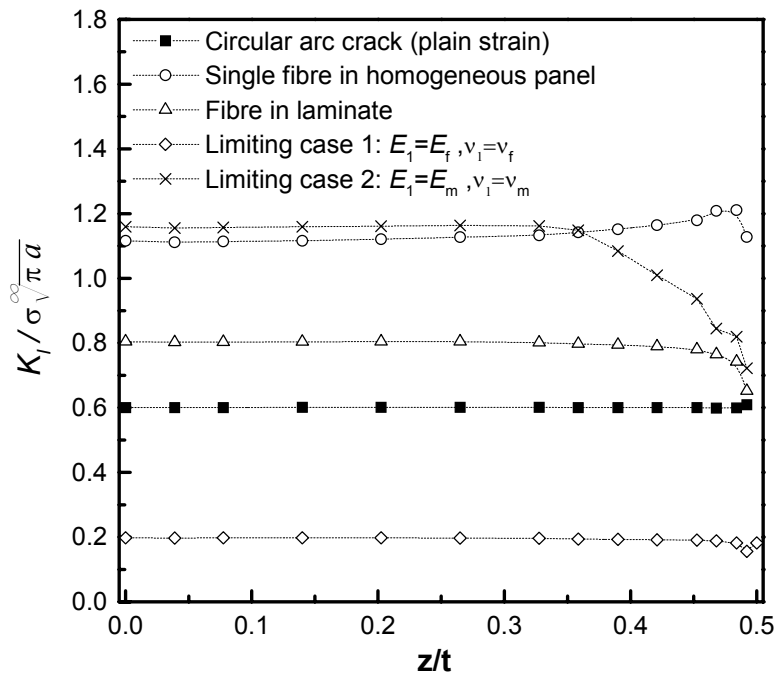
Figure 8: K_I along the crack front for the fibre/matrix interface crack
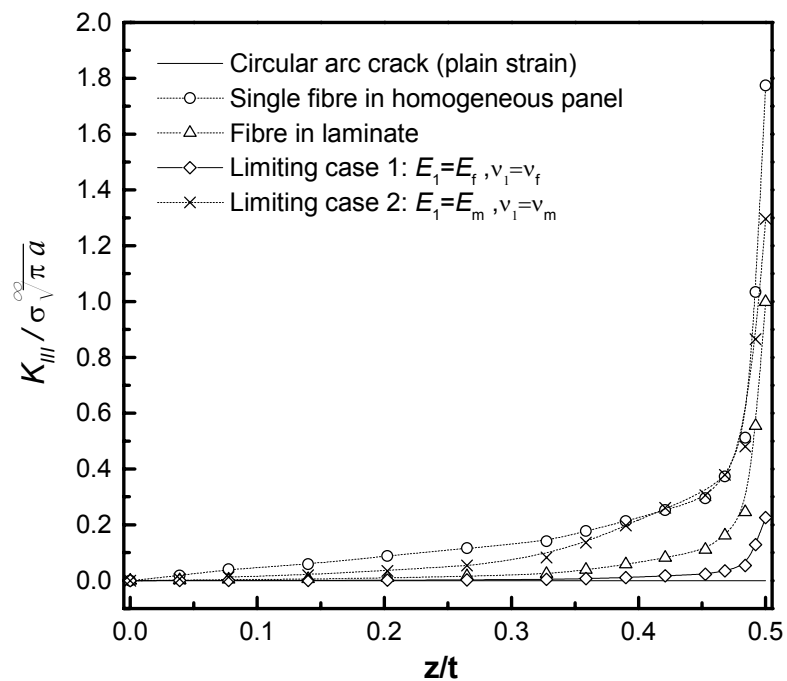
Figure 10: K_{II} along the crack front for the fibre/matrix interface crack

7 CONCLUSIONS

In this paper, a boundary element methodology for the three-dimensional analysis of bimaterial interface cracks has been presented.

The interface crack analysis is addressed using a multidomain BEM formulation in order to account for the different material properties at both sides of the crack. Fracture mechanics parameters, namely J-integral and stress intensity factors, are computed along the crack front using the Energy Domain Integral and the M_I-integral methodologies. These are implemented as a post-processing technique, and so it can be applied to the results from a particular model at a later stage. The implementation takes advantage of the efficiency of the boundary integral equation to directly obtain the required displacement derivatives, stress and strain fields from their boundary integral representations. The efficiency and accuracy of the proposed implementation is demonstrated by analysing a number of examples, and their results compared with those available in the bibliography.

The analysis of an application example consisting in interface crack formed after the fibre/matrix debonding closes the chapter. Obtained results show the key role played by the bimaterial properties and the three-dimensional effects in the state of mixed mode fracture. In view of determining the fracture behaviour, these effects are very critical since they influence not only the variation of energy release rate, but also all three modes of fracture along the crack front.

ACKNOWLEDGEMENTS

REFERENCES

[1] Aliabadi M.H. and Rooke D.P., *Numerical Fracture Mechanics*, Computational Mechanics Publications and Kluwer Academic Publishers, Dordrecht and Southampton (1992)

[2] Tan C.L. and Gao Y.L., "Treatment of bimaterial interface crack problems using the boundary element method", *Engineering Fracture Mechanics*, 36, 919-932 (1990)

[3] Yuuki R., and Cho S-B., "Efficient boundary element analysis of stress intensity factors for interface cracks in dissimilar materials", *Engineering Fracture Mechanics*, 34, 179-188 (1989)

[4] Mao R, and Sun G., "A study of the interaction between matrix crack and matrix-fibre interface", *Engineering Fracture Mechanics*, 51/3,469-477 (1995)

[5] He W.J., Lin D.S. and Ding H.J., "A boundary element for crack analysis at a bimaterial interface" , *Engineering Fracture Mechanics*, 49/3, 405-410 (1994)

[6] Miyazaki N., Ikeda T., Soda T. and Munakata T., "Stress intensity factor analysis of interface crack using boundary element method – Application of contour-integral method", *Engineering. Fracture. Mechanics*, 45/5, 599-610 (1993)

[7] de Paula F.A. and Aliabadi M.H., "Boundary element analysis of interface cracks in dissimilar orthotropic materials using path independent contour integral", *Boundary Elements XIX, 19th International Conference on the Boundary Element Method*, Computational Mechanics Publications, Southampton, UK (1997)

[8] Moran B. and Shih C.F. ,"A general treatment of crack tip contour integrals", *Int. J. Fracture*, 295-310, (1987)

[9] Cisilino A.P., Aliabadi M.H., and Otegui J.L., "Energy domain integral applied to solve center and double-edge crack problems in three-dimensions", *Theoretical and Applied Fracture Mechanics*, 29, 181-194 (1998)

[10] Chen F.H.K. and Shield R.T., "Conservation laws in elasticity of the *J*-integral type", *J. Appl. Math. Phys. (ZAMP)*, 28,1-22 (1977)

[11] Gosz M., Dolbow J. and Moran B., "Domain integral formulation for stress intensity factor computation along curved three-dimensional interface cracks", *Int. J. Solids and Structures*, 35/15, 1763-1783 (1998)

[12] Nagashima T., Omoto Y. And Tani S., "Stress intensity factor analysis of interface cracks using X-FEM", *Int. J. Num. Meth. Engng.*, 56,1151-1173 (2003)

[13] Im S., Kim H-G., and Kim Y.J., "Mode decomposition of three-dimensional mixed-mode cracks via two-state integrals", (to appear)

[14] Williams M.L., "The stress around a fault or crack in dissimilar media", *Bulletin of the Seismological Society of America*, 49, 199-024 (1959)

[15] Rice J.R., Suo Z., and Wang J.S., "Mechanics and Thermodynamics of Brittle Interfacial Failure in Bimaterial Systems", *Metal-Ceramics Interfaces*, M.Ruhle et al., Eds, Pergamon Press, 269-294 (1990)

[16] Dundurs J., "Edge-bonded dissimilar orthogonal elastic wedges under normal and shear loading", *ASME Journal of Applied Mechanics*, 36, 650-652 (1969)

[17] Shih C.F., Moran B., and Nakamura T., *Int. J. of Fracture*, 30, 79-102 (1986)

[18] Xie M., and Chaudhuri R.A., "Three-dimensional stress singularity at a bimaterial interface crack front", *Composite Structures*, 40/2, 137-147, (1998)

[19] Meurs Paul, Characterization of Microphenomena in Transversely Loaded Composite Material, PhD Thesis, Technische Universiteit Eindhoven, (1998)